Available online at www.sciencedirect.com
SCIENCE DIRECT®
Aquatic Living Resources 16 (2003) 95–103
Aquatic Living Resources
www.elsevier.com/locate/aquliv

Microstructure, nanostructure and composition of the shell of *Concholepas concholepas* (Gastropoda, Muricidae)

Yannicke Dauphin [a,*], Nury Guzman [b], Alain Denis [a], Jean-Pierre Cuif [a], Luc Ortlieb [b]

[a] *Département des sciences de la terre, bât. 504, Université Paris XI-Orsay, 91405 Orsay cedex, France*
[b] *UR055 paléotropique, IRD, 32 av. H. Varagnat, 93143 Bondy cedex, France*

Received 29 November 2002; accepted 23 January 2003

Abstract

Among the gastropods, some muricid shells are composed of an inner aragonitic crossed lamellar layer and a calcitic prismatic outer layer. The analysis of the structure and composition of the two layers of *Concholepas* shows that the crossed lamellar layer is similar to those of other Mollusc taxa. Sr, Mg and S contents are low in both layers. According to infrared spectrometry, the organic content of the outer calcitic layer is higher than that of the aragonitic crossed lamellar layer. The study of the nanostructure allows for the proposal of a new 3D interpretation of the fine structure of the crossed lamellar layer. The calcitic prismatic layer is compared with the outer calcitic prismatic layer of an archaeogastropod genus: *Haliotis*.

Résumé

Microstructure, nanostructure et composition de la coquille de *Concholepas concholepas* (Gastéropode, Muricidés). Parmi les Gastéropodes, quelques Muricidés ont une coquille formée par une couche interne aragonitique à structure lamellaire croisée, et une couche externe calcitique prismatique. L'analyse de la structure et de la composition des deux couches de la coquille de *Concholepas* montre que la couche lamellaire croisée est similaire à celle des autres Mollusques. Les teneurs en Sr, Mg et S sont faibles dans les deux couches. Selon les spectres infrarouges, le contenu en composants organiques est plus élevé dans la couche externe calcitique que dans la couche interne aragonitique. L'étude des nanostructures de la couche aragonitique a permis de proposer un nouveau modèle de la structure lamellaire croisée. La couche prismatique externe est comparée à celle d'un archéogastéropode : *Haliotis*.

Keywords: Microstructure; Composition; Shell; Muricidae; *Concholepas*

1. Introduction

Concholepas concholepas, also called south pacific abalone, is a carnivorous muricid gastropod, typical from the waters of Peru and Chile. There has long been a small local market for Loco (the Spanish name for *Concholepas*), and intertidal harvesting is still commonplace. The commercial export market began in 1976. *Concholepas*, the single most economically important shellfish in Chile, has been overexploited. Demand was so high that the government closed the fishery from 1989 to 1992. Another interest was due to the haemocyanin (an immunogenic protein), isolated and purified from the lymph of *Concholepas*. Several projects including culture, population studies in protected zones and comparison of larval behaviours in natural and artificial settlements have shown the role of human predation, climate and environmental factors on the abundance of *Concholepas* (Rodriguez et al., 1995; Moreno et al., 1998; Manriquez and Castilla, 2001; Poulin et al., 2002).

It is well known that mollusk shells have a high environmental significance and provide information on physiological events (duration of spawning period, growth, etc.); moreover, they are clearly related with taxonomy and phylogeny. However, few data are available on the structure and composition of the shell of *Concholepas*.

* Corresponding author.
E-mail address: dauphin@geophy.geol.u-psud.fr (Y. Dauphin).

DOI: 10.1016/S0990-7440(03)00022-6

In the first extensive study of molluscan shell structures, (Boggild 1930) described and classified the main categories from mineralogical, crystallographic and microstructural characters. The most widespread structure was the aragonitic crossed lamellar layer. However, distinctive microstructural and mineralogical features were noticed in different families. Some Muricidae showed an unusual association of several aragonitic crossed lamellar sublayers and an outer thin layer of "longitudinal lamellae" (1930: p. 314). Despite this promising beginning, studies were mainly directed towards bivalve shells in subsequent decades (Taylor et al., 1969, 1973; Kobayashi, 1969, 1980; Kobayashi and Akai, 1994). (Petitjean, 1965) worked on the structural, mineralogical, and chemical characteristics of the Muricids, and was interested in finding characters that could be useful in systematics. His work included observations of ultra thin shell sections, but no electron microscopy. The author recognized a calcitic "cortex" in various species, and an aragonitic "ostracum"; he used the presence or absence of a calcitic cortex as a subfamilial taxonomic characteristic. For example, the Rapaninae have a cortex, while the Muricinae do not. In *C. concholepas*, the calcitic cortex was always found, and this species was thus assigned to the subfamily Rapaninae.

The aim of this paper is to study the micro- and nanostructures, as well as the chemical composition of the shell of gastropod *C. concholepas* by using microscopic, energy dispersive spectroscopy (EDS) and infrared spectroscopy (FTIR) analyses.

2. Material and methods

2.1. Material

C. concholepas (Bruguière, 1789): class Gastropoda, Orthogastropoda. Caenogastropoda, Sorbeoconcha, Hypsogastropoda, Neogastropoda.

Muricoidea Rafinesque, 1815; Muricidae Rafinesque, 1815; Rapaninae Gray, 1853.

Samples of adult *C. concholepas* were collected by local fishermen in the Antofagasta area (Santa Maria Island, Chile) at a maximal depth of 5 m. The soft parts of the animal were removed and shells were rinsed with seawater, and then with tap water.

2.2. Methods

2.2.1. Light microscopy

First insights were obtained by observing thin (~40 μm) and ultra-thin (~5 μm) sections of longitudinal and transversal plans of shell ridges, with both normal and crossed nicols light microscopy.

2.2.2. Scanning electron microscopy

Fractures and polished sections were prepared. Polished sections and some fractures were etched with various acid solutions and enzymes to reveal microstructural features. Fixative and etching solutions such as a mixture of acetic acid 1% + glutaraldehyde 12% were used to preserve the organic matrices. These matrices were partially destroyed by enzymes at 38 °C under a gentle rocking (Alcalase—Merck, 1 mg/ml Protease—Sigma in HEPES pH 7.8, 1 mg/ml Trypsine—Sigma in HEPES pH 7.8) to reveal the shape of microcrystals. Basic pH was used to minimize the dissolution of the carbonate of the shell. Scanning electron microscopy (SEM) observations were conducted with Philips SEM 505 and XL30 microscopes housed at the Laboratoire de géologie, Université d'Orsay— Paris XI.

2.2.3. Atomic force microscope

Scanning probe microscopy encompasses a family of techniques that measures surface topography and properties at the atomic scale. The atomic force microscope (AFM) maps the topography of surface. In phase imaging, a variant of tapping mode, the phase lag of the cantilever oscillation relative to the signal sent to the cantilver's piezo driver is used as a basis for image generation. Phase images can be generated as a consequence of variations in material properties such as friction, viscoelasticity, and adhesion. AFM observations were conducted with Digital Instruments (Veeco) Nanoscope III Dimension 3100 (Université d'Orsay), at room temperature and air. The probe consisted of a cantilever with integrated Si_3N_4 tips (Digital Instruments). Micron scale images were acquired by using the tapping mode. The procedures of the sample preparations are given in the figure legends.

2.2.4. Energy dispersive spectroscopy

Chemical analyses were done on an electron microprobe by EDS. Energy dispersive X-ray microanalysis was undertaken with a Cambridge Stereoscan 200 SEM, equipped with a solid-state X-ray detector. Quantitative analysis was done using the Link AN10000 analysis system by a ZAF/PB program that estimates peak-to-background ratios (IRD, Bondy). Samples were embedded in resin and polished with diamond pastes. The surface was then lightly etched in 5% formic acid for 15 s to reveal anystructural details within the samples (e.g. different layers), so that the analysis positions could be related to any observed structural features. Measurements were made using a lifetime of 100 s. Operating conditions were an accelerating voltage of 15 kV. A cobalt standard provided the instrument calibration.

Elements analysed were Ca, Na, Mg, Sr, Al, S, P, K, Fe, and Mn. Minimum of 10 analyses were made at various locations on each layer of each shell (5). These punctual analyses have been averaged to obtain an individual mean.

2.2.5. Infrared spectrometry

First, the epibionts found in the outer surface of the shells were mechanically removed. Then the two layers of the cleaned *C. concholepas* shells were separated. The small pieces obtained were immersed in 3% NaClO to remove organic contaminants, rinsed with Milli-Q water, dried, and

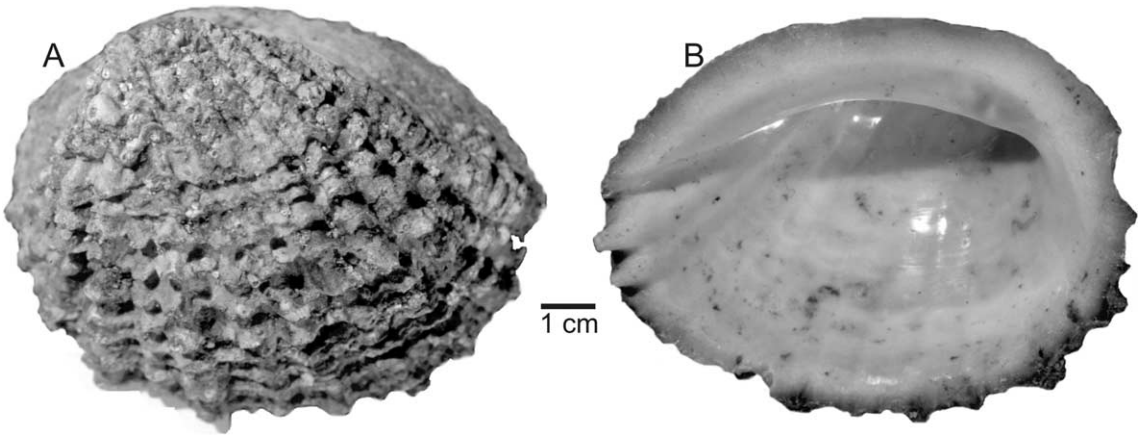

Fig. 1. Outer (A) and inner (B) views of the shell of *C. concholepas*.

ground into powder. The powdered samples were dried in an oven at 38 °C for one night. All spectra were recorded at 4 cm^{-1} resolution with 64 scans using a strong Norton-Beer apodization on a Perkin Elmer model 1 600 Fourier transform infrared spectrometer (FTIR) from 4000 to 450 cm^{-1}. The spectrometer was equipped with a diffuse reflectance accessory, which permits DRIFT measurements with high sensitivity on powders. All spectra were corrected by using the Kubelka-Munk function.

3. Observations

C. concholepas has a thick, round and white-gray shell (Fig. 1) (Guzman et al., 1998, 2001). The outer surface of the shell, often encrusted with epibionts such as small barnacles, shows strong lamellose ribs (Fig. 1A). The smooth and glossy inner surface of the shell is white (Fig. 1A).

3.1. Micro- and nanostructures

Thin sections show that the shell is composed of two main layers (Fig. 2a–d). The thickness of the shell near the apex is about 1620 μm (calcite = 480 μm, aragonite = 1140 μm) and 2250 μm near the pallial margin (calcite = 2130 μm, aragonite = 120 μm). Depending on the presence/absence of the outer ridges, the thickness is variable. The calcitic outer layer is thin near the apex (Fig. 2a) but becomes thicker towards the pallial margin (Fig. 2c–d). The aragonitic inner layer is subdivided into several sublayers (Fig. 2a,e), and becomes very thin near the growing edge of the shell (Fig. 2c–d).

Thin sections of the calcitic outer layer show numerous growth lines in large crystals (Fig. 2a, C–D), with longitudinal axes oblique or perpendicular to the shell surface (Fig. 2b). This structure has been called prismatic (Boggild, 1930). These “prisms” do not show regular polygonal sections, and they do not have regular diameter. In most of the shell, the size of the prisms increases from the outer surface to the crossed lamellar layer (Fig. 2a–d). The thin sections also show that the extinctions of adjacent prisms are not simultaneous under crossed nicols (Fig. 2a,b,d). The SEM micrographs confirm that the growth lines are well developed (Fig. 3a,b), and the prismatic units are irregular (Fig. 3b,c). Prisms are composed of small acicular crystallites (length about 2 μm) more or less perpendicular to the growth lines (Fig. 3c,d). AFM micrographs also show the irregularity of the components. Several etchings were used, but the acicular crystallites are not regularly visible in height (=topographic) images (Fig. 3f–g). Phase images, more sensitive to the composition of the sample, are more explicit. Acicular crystallites are composed of smaller units, aligned in small rows (Fig. 3g,i). Each unit is surrounded by a thin dark layer in image phase (Fig. 3i), whereas no layer is seen in a height image. It is suggested that the thin layer is composed of organic matrix. The size of the smaller units varies from 15 to 140 nm (Fig. 3g,i). Three-dimensional images of the calcitic layer show more or less regular alignment of the crystallites (Fig. 4a–b). According to the orientation of the crystallites relative to the sections, the rows are more or less visible. The parallel rows in Fig. 3g are more visible in a 3D image (Fig. 4b).

The aragonitic inner layer is composed of crossed lamellar sublayers (Fig. 2a,e). The basic structures of each sublayer are similar; only the orientation of the units changes, a common feature of the crossed lamellar shells. The width of the first order lamellae is about 10 μm or more (Fig. 5a). Each lamella is composed of stacked second order lamellae (Fig. 5a), which size is approximately 1.2 μm. The complex structure of the second order lamella is visible in the SEM (Fig. 5a) and AFM (Fig. 5b,c) micrographs. The third order units have different orientations in two contiguous second order lamellae. Then third order lamellae are composed of smaller or fourth order elongated units: width 105 nm, length 630 nm (Fig. 5d,e). Phase image shows the change of orientation of the fourth units in contiguous third order lamellae (Fig. 5e,g). 3D images of similar zones show the fourth lamellae as elongated crystallites (Fig. 4c–d). This change in orientation in contiguous units is a constant characteristic of the crossed lamellar structure (Fig. 6). Thus, according to the fracture plane, lamellae seem to be elongated or rounded units (Fig. 5f,g). The fourth order lamella is also a composite

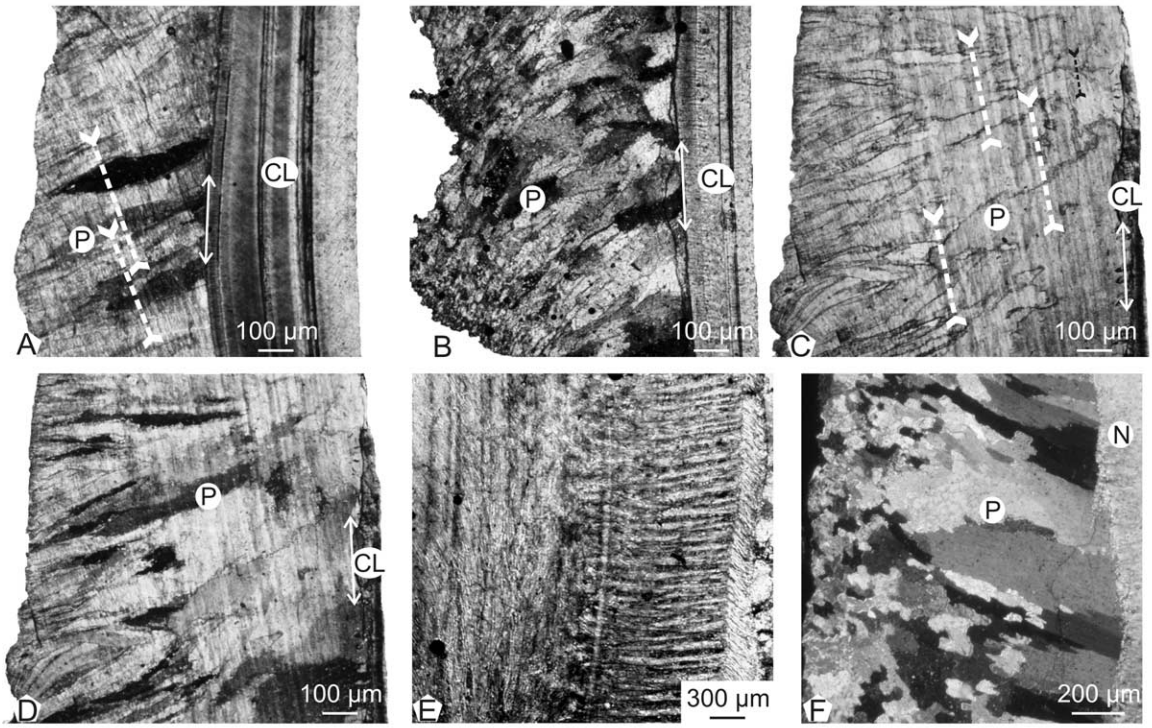

Fig. 2. (a–f) Thin sections of *C. concholepas*. (a) External calcitic layer (P) and crossed lamellar layer (CL) near the apex. Growth lines are present in the prismatic layer (dotted arrows). Crossed nicols. (b) External calcitic layer (P) and crossed lamellar layer (CL) in the middle region of the shell. The prisms are large in the inner part of the layer and small in the outer part. Crossed nicols. (c) External calcitic layer (P) and crossed lamellar layer (CL) near the pallial edge. (d) Idem, crossed nicols. (e) Detail of the sublayers of the crossed lamellar layer. Crossed nicols. (f) *Haliotis*: outer calcitic prismatic layer (P) and aragonitic nacreous layer (N). Crossed nicols.

structure, as shown by the phase images (Fig. 5h–i). The dark layer surrounding the units may be indicative of an organic composition. The width of a granule is approximately 42 nm.

3.2. Bulk composition

The infrared spectra of the calcite and aragonite groups are characterized by three major bands attributed to the carbonate radical CO_3^{2-}: ν3 at 1429 cm^{-1}, the ν2 doublet 877–848 cm^{-1}, and ν4 at 713 cm^{-1} for the calcite group; ν3 at 1 471 cm^{-1} and two doublets: ν2 at 877–848 cm^{-1} and ν4 at 713–700 cm^{-1} for the aragonite group (Adler and Kerr, 1962, 1963; Farmer, 1974; Jones and Jackson, 1993). A comparison between chemical compositions and FTIR data shows that there is a linear correlation between the Mg and Sr contents and the wavelength of some FTIR bands. In aragonite, there is a negative correlation between the ν2 wavelengths and the Sr contents, and a negative correlation between ν2 wavelengths and the Mg contents (Dauphin, 1997): a part of this doublet varies from 863.7 to 858.8 cm^{-1}. The other part (844 cm^{-1}) of this doublet is not altered. In biogenic calcite, there is a positive linear correlation between the ν4 wavelength and Mg concentrations (Dauphin, 1999).

The spectra of the powdered outer layer confirm the calcitic mineralogy (Fig. 7): the ν2 doublet 877–848 cm^{-1}, ν1 at 1013 cm^{-1} and ν4 at 713 cm^{-1}. However, the ν3 band is subdivided: 1457, 1445 and 1436 cm^{-1}. Other bands usually present in calcite are also visible: 1176 and 1084 cm^{-1}. The ν2 wavelength is indicative of low Mg and Sr contents of the layer (<1000 ppm). Several other bands may be attributed to the organic matrix: 3274 cm^{-1} band may be assigned to amide A, 1685–1653–1636 cm^{-1} bands to the amide I.

The thin inner layer is aragonitic (Fig. 7). However, the ν3 band is also subdivided (1492 and 1458 cm^{-1}), and only one band of the ν2 is seen at 863 cm^{-1} and ν1 is seen at 1083 cm^{-1}. This wavelength is indicative of low Sr (<2500 ppm) and Mg (<800 ppm) contents. The amide A band is at 3310 cm^{-1}, and the amide I region is composed of two bands (1654 and 1636 cm^{-1}).

To estimate the organic/mineral ratio from FTIR spectra, two ratios are used: amide I/860, and amide A/860 for aragonitic layers (Dauphin and Denis, 2000). The first ratio is equal to 0.14 and the second one to 0.08 in the crossed lamellar layer. In calcitic layers, the 878 cm^{-1} band was used and the ratios are 0.23 and 0.07, respectively. According to these data, the organic content of the outer calcitic layer is higher than that of the aragonitic crossed lamellar layer.

3.3. Chemical composition (EDS data)

The outer prismatic calcitic layer shows a low minor element content, including Mg (Fig. 8). In fact, Mg content is lower than Sr. K and Mn contents, usually correlated with calcite, are also low. Aragonitic crossed lamellar layers are known to have low minor element contents, and *Concholepas* is not different (Fig. 8). The Loreau ratio (1982) is in the

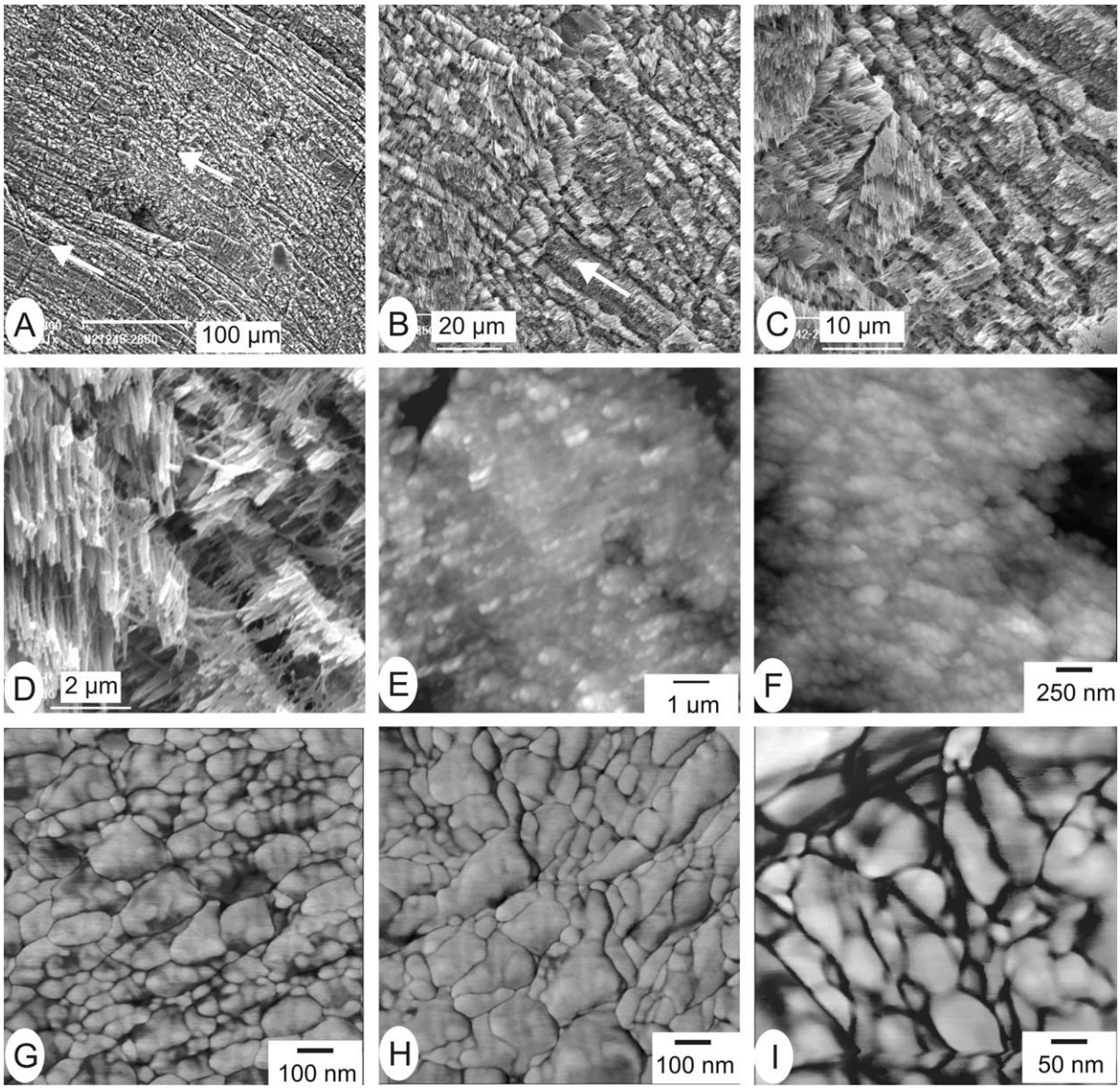

Fig. 3. Polished and etched sections of the calcitic external layer. (a) The large prisms seen in transmitted microscopy are not visible, whereas the growth lines are parallel (arrows). Acetic acid 1% + glutaraldehyde 12% for 12 min, SEM. (b–d) Detail of the same region, showing small acicular crystallites perpendicular or oblique relative to the growth lines, SEM. (e) Acicular crystallites in the growth layers near the pallial edge. Compare with (d). Alcalase, 23 h, AFM height image. (f) Acicular crystallites composed of aligned small units. Protease, 23 h, AFM height image. (g) Both small and large crystallites surrounded by a thin dark organic layer. Milli-Q water, 20 °C, 16 h, AFM image phase. (h) The alignment, size and shape of crystallites are better seen in phase image. Milli-Q water, 20 °C, 16 h. (i). Detail of crystallites with their outer dark envelope. These crystallites seem to be composite. Trypsine, 23 h, AFM phase image.

lower part of the aragonitic range: $L = 0.71$. It must be added that the Sr contents are similar in the calcitic and aragonitic layers, whereas Na content is higher in the aragonitic one.

4. Discussion and conclusion

4.1. Structure

C. concholepas is a neogastropod, and because of its unusual shell morphology, it is often compared with the archaeogastropod *Haliotis*. It must be noted that *Haliotis* has also a "succulent" meaty body and that its haemocyanins are used for its immunogenic properties. *Haliotis* shell is composed of an inner aragonitic layer, and an outer layer. Depending on the species, the outer prismatic layer is either calcitic, aragonitic or consists of a mixture of aragonite and calcite. The inner layer is nacreous, a structure never seen in *Concholepas*, whereas the crossed lamellar structure is not known in *Haliotis* (Dauphin et al., 1989).

Since (Boggild, 1930), the outer layer of most muricid shells is called prismatic. However, this structure is very different from that of the large polygonal parallel prisms of bivalve shells such as *Pinna* or *Pinctada* (Cuif et al., 1983, 1985). The calcitic prismatic layer of *Concholepas* is similar to that of the *Haliotis* shell (Dauphin et al., 1989). As for

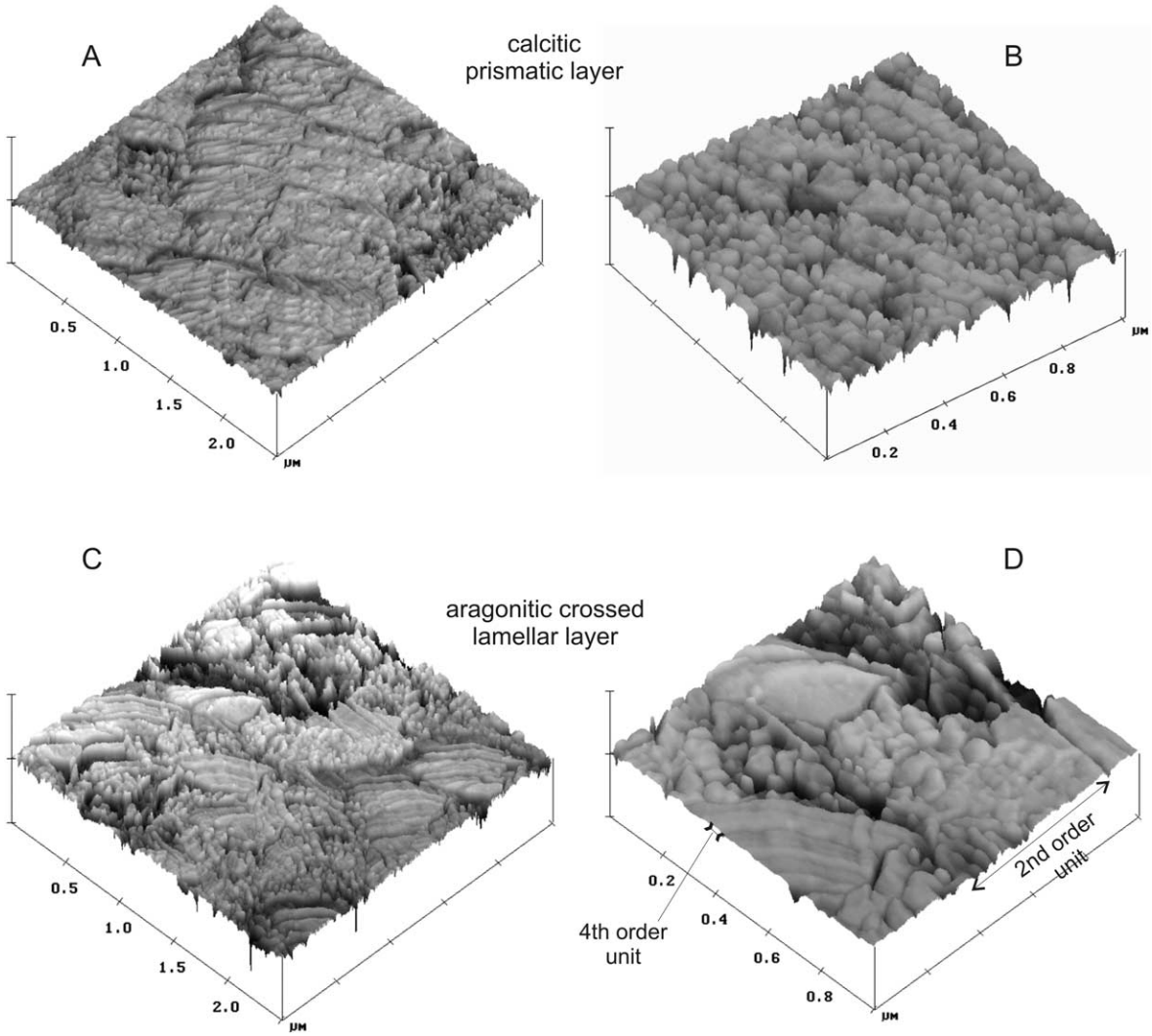

Fig. 4. (a–b) Polished and etched section showing the size and arrangement of the small acicular calcitic crystallites. Milli-Q water, 20 °C, 16 h. (c–d) Same sample, showing the various shapes of the third order units of the aragonitic crossed lamellar layer according to the sections, and their complex internal structure. AFM image phase.

Concholepas, the size of the prisms decreases from the inner part to the outer part of the layer (Fig. 2f).

The structure of the crossed lamellar layer is similar in bivalve and gastropod shells, and several 3D graphs have been proposed since Boggild (1930). The width of the first order lamellae varies from 10 to 30 µm. The minimal length of third order units is about 5 µm, and their width is between 0.3 and 2 µm (Uozumi et al., 1971). The various units of the *Concholepas* layer show similar sizes. Uozumi et al. (1971: p. 452) noticed that the third order lamella are subdivided in smaller units "parallel to the longitudinal axes of the crystals". They also described oblique regular dark stripes, supposed "to reflect the lattice structures of aragonite crystals". However, these minute structures are not illustrated. According to the SEM observations, it has been supposed that a third order lamella was divided in small fourth order cubes (Cuif et al., 1985; Dauphin and Denis, 2000). However, our AFM observations have shown that the third order lamellae are longitudinally divided, as are the fourth and fifth order units (Fig. 6). Each subdivision is perpendicular to the previous one as seen in a transverse plane, but parallel to the longitudinal axis of the unit. The question of a transverse striation all along the length of the fifth or sixth order units is not yet resolved.

4.2. Composition

FTIR analyses on mollusc shells are scarce, and no data are available on calcitic prismatic structures similar to the outer layer of *Concholepas*. FTIR spectra of the crossed lamellar layers of the gastropods *Cypraea*, *Phalium* and *Strombus* are similar and are also indicative of low Sr and Mg contents. However, these genera differ in their organic bands: the ratios calculated from FTIR spectra to estimate the organic contents vary from 0.20 to 0.33 (amide I/860), and from 0.07 to 0.19 (amide A/860) (Dauphin and Denis, 2000). Thus, the organic/mineral ratio of the crossed lamellar layer of *Concholepas* seems low, despite the paucity of data.

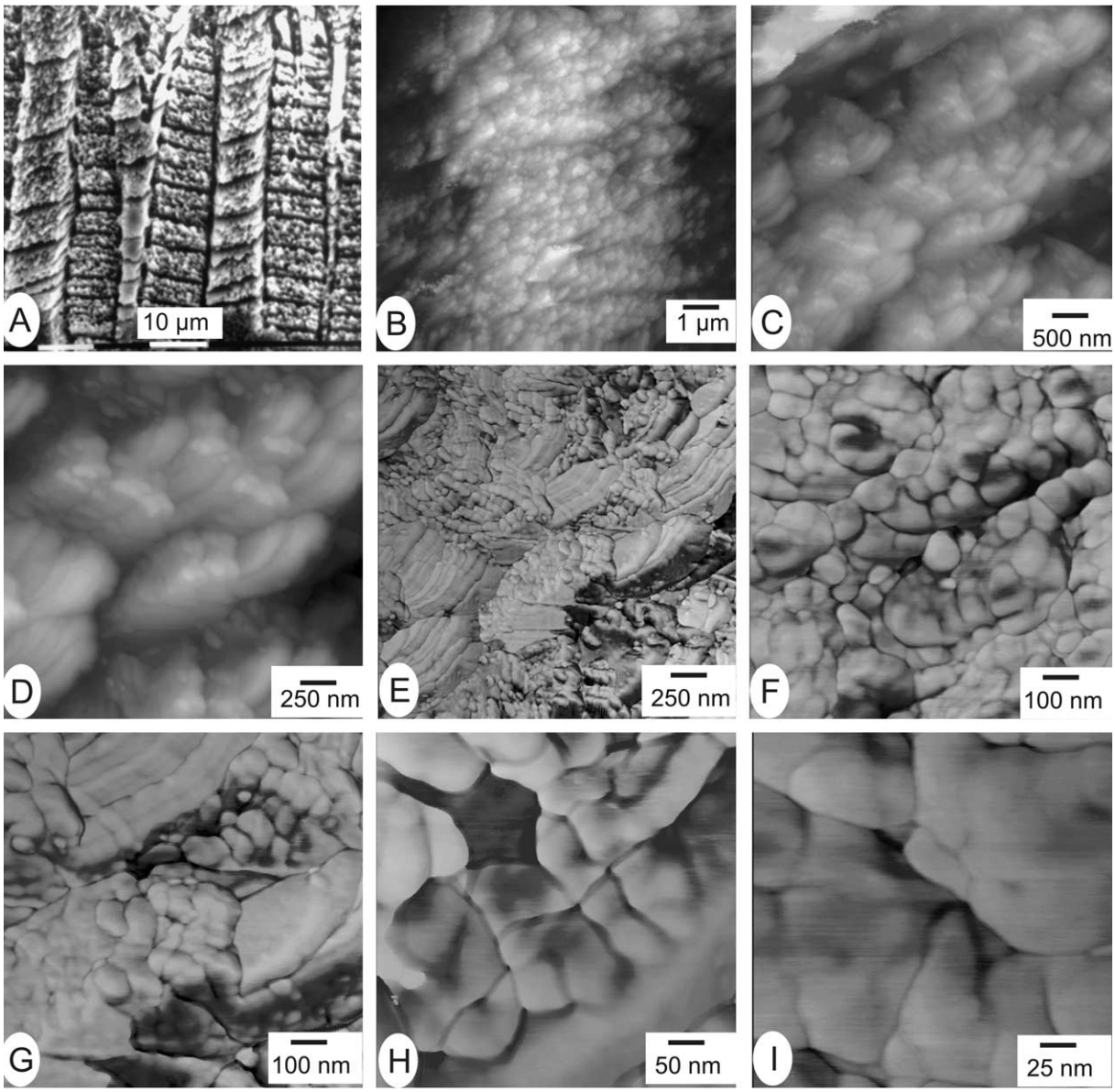

Fig. 5. Aragonitic crossed lamellar layer. (a) First order lamellae (vertical units) composed of second order lamellae. Polished and etched surface: formic acid 10%, 10 s, SEM. (b) Polished and etched section showing a first order lamella with crystallites of the second order lamellae. Milli-Q water, 16 h, 20 °C, AFM height image. (c) Detail of (b), showing the complex structure of a second order lamella. (d) Detail of (c), showing the heterogeneous third order lamellae. (e) AFM image phase of (d). (f) Fourth order lamellae. Same preparation, AFM phase image. (g) Heterogeneity of the fourth order elements and their different shapes according to the orientation of the section, AFM phase image. (h) Fourth order units are subdivided. Same preparation, AFM phase image. (i) Detail of the structure of the fourth order units. Polished surface. Protease, 23 h, AFM phase image.

The calcitic prismatic layers of various *Haliotis* species show moderate variations (Dauphin et al., 1989). Mg contents of *Concholepas* are lower than those of *Haliotis*, whereas other element contents are similar (Fig. 8A). The Sr contents of the crossed lamellar layer of *Concholepas* are lower than 2000 ppm, and similar to those of other aragonitic crossed lamellar layers of gastropod shells (Fig. 8B). All the aragonitic layers of mollusc shells have a low minor element content, Sr included (Harriss, 1965; Masuda, 1976; Masuda and Hirano, 1980; Turekian and Armstrong, 1960; Dauphin and Denis, 2000).

The shell of *C. concholepas* is an unusual arrangement of an outer calcitic prismatic layer and an inner aragonitic crossed lamellar layer, with different quantities of organic matrix. Despite this pattern, the structure and the chemical composition of each layer are in the range of the mollusc shells. The holes drilled by *Octopus* in the *Concholepas* shell have a restricted area (Cortez et al., 1998): the apex zone is the thinnest part of the shell, and the aragonite/calcite thickness ratio is high. The mechanical properties of the shell layers are not well known, and it has been shown that the crystal size and proportion of organic matrix play a major role (Harper, 2000).

Numerous studies estimated the growth of wild and cultured specimens based on the length and weight of the animals (Rodriguez et al., 2001). Another approach is based on

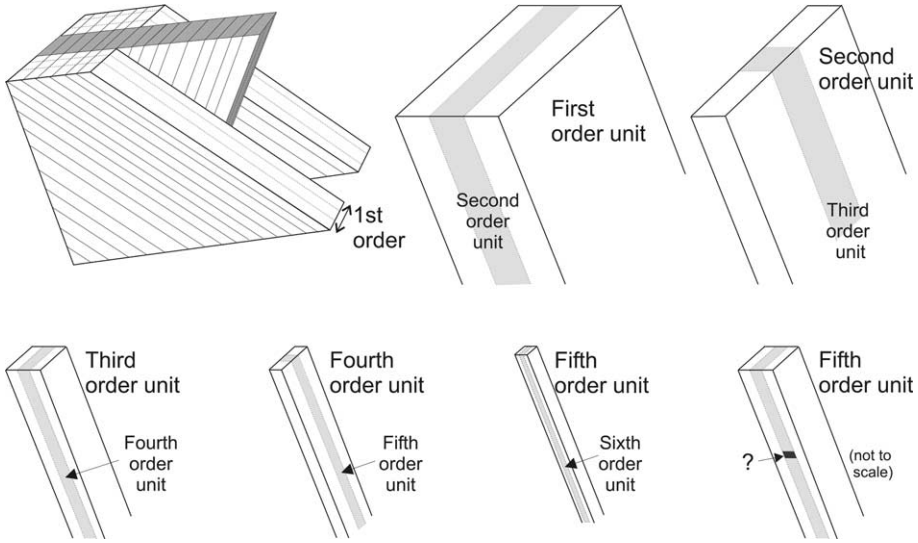

Fig. 6. Schematic reconstruction of the crossed lamellar layer.

the growth lines. The pattern of growth lines and the chemical contents of shells record various events such as temperature changes, toxic blooms, pollution, etc. (Lorrain et al., 2000; Schöne et al., 2002). Few data on gastropod shells are yet available, but microscopic growth increments are clearly visible in the calcitic layer of *Concholepas*. By using statistical methods developed by dendrochronologists, environmental data should be extracted from the growth lines in the shell of *Concholepas*. A combination of microincrement counts, in situ temperature and/or salinity monitoring, and localized chemical analyses must provide precise data on the growth and biology of wild animals. The information will lead to the improvement of the techniques of culture, the management of wild *Concholepas*, and thus reduce the "predation" pressure of the wild animals.

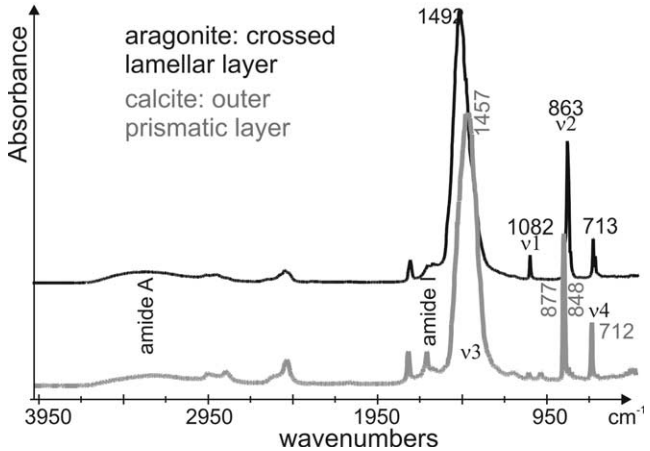

Fig. 7. FTIR spectrum of the two layers of *C. concholepas*, showing their different mineralogy and the low contents of organic matrix.

Acknowledgements

The authors would like to thank S. Caquineau (US094, Géosciences de l'Environnement Inter-tropical, IRD Bondy) for helping to obtain microprobe analyses on *Concholepas*. This work was made possible with the financial support of PNEDC program of INSU-CNRS.

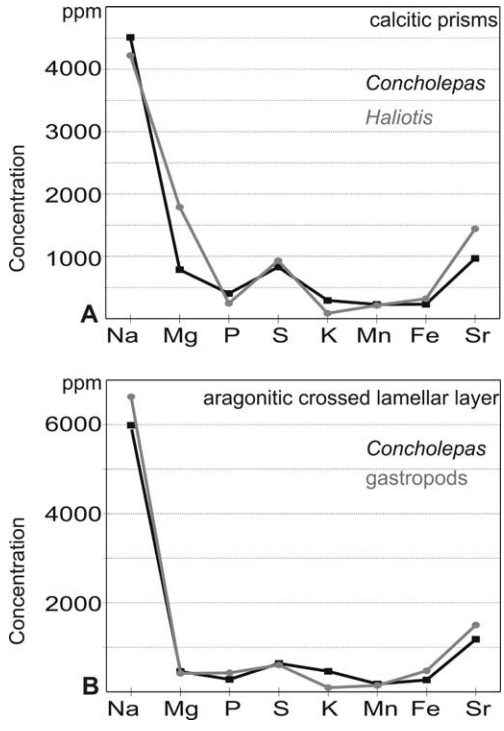

Fig. 8. Minor element contents of the calcitic prisms (A) and aragonitic crossed lamellar layers (B) of *C. concholepas*, *Haliotis*, and various gastropod shells.

References

Adler, H.H., Kerr, P.F., 1962. Infrared study of aragonite and calcite. Am. Mineral. 47, 700–717.

Adler, H.H., Kerr, P.F., 1963. Infrared spectra, symmetry and structure relations of some carbonate minerals. Am. Mineral. 48, 839–853.

Boggild, O.B., 1930. The shell structure of the Mollusks. Kong. Dsk. Vidensk. Selsk. Skr., Natur. Math. Afd. 9, II 2, 230–326.

Cortez, T., Bernardino, G., Castro, B.G., Guerra, A., 1998. Drilling behaviour of *Octopus mimus* Gould. J. Exp. Mar. Biol. Ecol. 224, 199–203.

Cuif, J.P., Denis, A., Raguideau, A., 1983. Observations sur les modalités de mise en place de la couche prismatique du test de *Pinna nobilis* L. par l'étude des caractéristiques de la phase minérale. Haliotis 13, 131–141.

Cuif, J.P., Denis, A., Triclot, M.P., 1985. Ultrastructure de la couche externe du test d'un Veneracea: *Dosinia ponderosa* (Gray, 1838) (Mollusque, Lamellibranche). Bull. Mus. Natl. Hist. Nat. Paris 4è sér., Sect. A 4, 741–759.

Dauphin, Y., 1997. Infrared spectra and elemental composition in recent carbonate skeletons: relationships between the n2 band wavelength and Sr and Mg concentrations. Appl. Spectr. 51, 141–152.

Dauphin, Y., 1999. Infrared spectra and elemental composition in recent biogenic calcites: relationships between the n4 band wavelength and Sr and Mg concentrations. Appl. Spectr. 53, 184–190.

Dauphin, Y., Denis, A., 2000. Structure and composition of the aragonitic crossed lamellar layers in six species of Bivalvia and Gastropoda. Comp. Biochem. Physiol. A126, 367–377.

Dauphin, Y., Cuif, J.P., Mutvei, H., Denis, A., 1989. Mineralogy, chemistry and ultrastructure of the external shell-layer in ten species of *Haliotis* with reference to *Haliotis tuberculata* (Mollusca: Archaeogastropoda). Bull. Geol. Inst. Univ. Uppsala N.S. 15, 7–38.

Farmer, V.C., 1974. The infrared spectra of minerals. Mineral. Soc. Monogr. 4, London.

Guzman, N., Cuif, J.P., Ortlieb, L., 2001. Analisis Microestructural de la concha de *Concholepas concholepas* (Bruguière 1789) en una perspectiva de reconstitucion paleoambiental. XXI Congreso de Ciencias del Mar, Via del Mar. Chile 47, 1789.

Guzman, N., Saa, S., Ortlieb, L., 1998. Catalogo descriptivo de los moluscos litorales (Gastropoda y Pelecypoda) de la zona de Antofagasta, 23 S, Chile. Estud. Oceanol. Univ. Antofagasta 17, 17–86.

Harper, E.M., 2000. Are calcitic layers an effective adaptation against shell dissolution in the Bivalvia? J. Zool. 251, 179–186.

Harriss, R.C., 1965. Trace element distribution in molluscan skeletal material. I. Magnesium, iron, manganese, and strontium. Bull. Mar. Sci. 15, 265–273.

Jones, G.C., Jackson, B., 1993. Infrared Transmission Spectra of Carbonate Minerals. Chapman and Hall, London.

Kobayashi, I., 1969. Internal microstructure of the shell of bivalve molluscs. Am. Zool. 9, 663–672.

Kobayashi, I., 1980. Various patterns of biomineralization and its phylogenetic significances in bivalve mollusks. In: Omori, M., Watabe, N. (Eds.), The Mechanisms of Biomineralization in Animals and Plants. Tokai University Press, Tokyo, pp. 145–155.

Kobayashi, I., Akai, J., 1994. Twinned aragonite crystals found in the bivalvian crossed lamellar shell structure. J. Geol. Soc. Japan 100, 177–180.

Loreau, J.P., 1982. Sédiments aragonitiques et leur genèse. Mém. Mus. Natl. Hist. Nat. Paris N.S., sér. C, sciences de la terre 47, 1–312.

Lorrain, A., Paulet, Y.M., Chauvaud, L., Savoye, N., Nézan, E., Guérin, L., 2000. Growth anomalies in *Pecten maximus* from coastal waters (Bay of Brest, France): relationships with diatoms blooms. J. Mar. Biol. Assoc. UK 80, 667–673.

Manriquez, P.H., Castilla, J.C., 2001. Significance of marine protected areas in central Chile as seeding grounds from the gastropod *Concholepas concholepas*. Mar. Ecol. Prog. Ser. 215, 201–211.

Masuda, F., 1976. Strontium contents in shell of *Glycymeris*. J. Geol. Soc. Japan 82, 565–572.

Masuda, F., Hirano, M., 1980. Chemical composition of some modern marine pelecypod shells. Scient. Rep. Inst. Geosc. Univ. Tsukuba, Sect. B 1, 163–177.

Moreno, C.A., Asencio, G., Duarte, W.E., Marin, V., 1998. Settlement of the muricid *Concholepas concholepas* and its relationship with El Nino and coastal upwellings in southern Chile. Mar. Ecol. Prog. Ser. 167, 171–175.

Petitjean, M., 1965. Structure microscopique, nature minéralogique et composition chimique de la coquille de Muricidés (Gastéropodes, Prosobranches). Importance systématique de ces caractères. Thèse Faculté des Sciences de Paris. pp. 140.

Poulin, E., Palma, A.T., Leiva, G., Hernadez, E., Martinez, P., Navarrete, S.A., et al., 2002. Temporal and spatial variation in the distribution of epineustonic competent larvae of *Concholepas concholepas* along the central coast of Chile. Mar. Ecol. Prog. Ser. 229, 95–104.

Rodriguez, L., Daneri, G., Torres, C., Leon, M., Bravo, L., 2001. Modeling the growth of the Chilean loco, *Concholepas concholepas* (Bruguière, 1789) using a modified Gompertz-type function. J. Shellfish Res. 20, 309–315.

Rodriguez, S., Riquelme, C., Campos, E., Chavez, P., Brandan, E., 1995. Behavioral responses of *Concholepas concholepas* (Bruguière, 1789) larvae to natural and artifical settlement cues and microbial films. Biol. Bull. 189, 272–279.

Schöne, B.R., Lega, J., Flessa, K.W., Goodwin, D.H., Dettman, D.L., 2002. Reconstructing daily temperatures from growth rates of the intertidal bivalve mollusk *Chione cortezi* (northern Gulf of California. Mexico. Palaeogeogr. Palaeoclimatol. Palaeoecol. 184, 131–146.

Taylor, J.D., Kennedy, W.J., Hall, A., 1969. The shell structure and mineralogy of the Bivalvia. Introduction. Nuculacae–Trigonacae. Bull. Br. Mus. Natl. Hist. Zool. 3, 1–125.

Taylor, J.D., Kennedy, W.J., Hall, A., 1973. The shell structure and mineralogy of the Bivalvia–Lucinacea, Clavagellacea, conclusions. Bull. Br. Mus. Natl. Hist. Zool. 22, 255–294.

Turekian, K.K., Armstrong, R.L., 1960. Magnesium, strontium and barium concentrations and calcite-aragonite ratios of some recent molluscan shells. J. Mar. Res. 18, 133–151.

Uozumi,, S., Iwata,, K., Togo, Y., 1971. The ultrastructure of the mineral in and the construction of the crossed-lamellar layer in molluscan shell. Contr. Dept. Geol. Min., Fac. Sci. Hokkaido University 1236, pp. 447–455.